Elsevier Editorial System(tm) for Applied Catalysis B: Environmental
Manuscript Draft

Manuscript Number:

Title: TiO2/WO3-x composite coatings as efficient photocatalysts for degradation of organic poluttants

Article Type: Research Paper

Keywords: TiO2/WO3-x coatings;
Plasma electrolytic oxidation;
UV-vis photocatalysis;
Kinetics and mechanism

Corresponding Author: Dr. Zorana Dohčević-Mitrović, Ph.D.

Corresponding Author's Institution: Institute of physics Belgrade

First Author: Zorana Dohčević-Mitrović, Ph.D.

Order of Authors: Zorana Dohčević-Mitrović, Ph.D.; Stevan Stojadinović; Luca Lozzi; Sonja Aškrabić; Nataša Tomić; Novica Paunović; Saša Lazović; Sandro Santucci

Dear Editor,

Please, find enclosed our manuscript titled: "TiO_2/WO_{3-x} composite coatings as efficient photocatalysts for degradation of organic poluttants" by Zorana Dohčević-Mitrović et al., which we wish to be published as a regular paper in Applied Catalysis. B: Environmental.
The manuscript presents the investigation of structural, optical and photocatalytic performances of TiO_2/WO_{3-x} composite coatings for removal of different and harmful azo dyes from water under visible and UV irradiation. By using facile, relatively new and cost-effective synthesis method (Plasma electrolytic oxidation) we demonstrated that it is possible to produce TiO_2/WO_{3-x} coatings, which are much better photocatalists under visible and UV irradiation than pure TiO_2. These compounds exhibit much better light absorption and enhanced charge separation efficiency particularly under visible irradiation. This article is original, new and is not being considered elsewhere. We believe that our manuscript is suitable for publication in Applied Catalysis. B: Environmental.

Best regards

Zorana Dohčević-Mitrović

***List of Three (3) Potential Reviewers**

1. Wan In Lee
Department of Chemistry, Inha UniVersity, Incheon, 402-751 Korea
e-mail: wanin@inha.ac.kr

2. Xintong Zhang
Center for Advanced Optoelectronic Functional Materials Research, and Key Laboratory for UV-Emitting Materials and Technology of Ministry of Education, Northeast Normal University, 5268 Renmin Street, Changchun 130024, China
e-mail: xtzhang@nenu.edu.cn (X. Zhang).

3. Yahia Djaoued
Laboratoire de Recherche en Mate´riaux et Micro-spectroscopies Raman et FTIR, Universite´ de Moncton, Campus de Shippagan, Shippagan, NB, Canada
e-mail: Yahia.djaoued@umoncton.ca

TiO_2/WO_{3-x} composite coatings as efficient photocatalysts for degradation of organic poluttants

Zorana Dohčević-Mitrović[a*], Stevan Stojadinović[c], Luca Lozzi[d], Sonja Aškrabić[a], Nataša Tomić[a], Novica Paunović[a], Saša Lazović[b], Sandro Santucci[d]

[a]Center for Solid State Physics and New Materials, Institute of Physics Belgrade, University of Belgrade, Pregrevica 118, 11080 Belgrade, Serbia.
[b]Institute of Physics Belgrade, University of Belgrade, Pregrevica 118, 11080 Belgrade, Serbia.
[c]Faculty of Physics, University of Belgrade, Studentski Trg 12-16, 11000 Belgrade, Serbia
[d]Department of Physical and Chemical Sciences, University of L'Aquila, Via Vetoio 67100, L'Aquila, Italy

Corresponding author. Tel.: +381113713024; Fax: +381113162190.
E-mail address: zordoh@ipb.ac.rs

Abstract

TiO_2/WO_{3-x} composite and pure TiO_2 coatings were prepared on titania substrates using facile and cost-effective plasma electrolytic oxidation process. The obtained samples were characterized by X-ray diffraction (XRD), scanning electron microscopy (SEM), Raman spectroscopy and UV-vis diffuse reflectance spectroscopy. The photocatalytic efficiency of pure TiO_2 and TiO_2/WO_{3-x} samples was evaluated by performing the photodegradation experiments in an aqueous solution of Rhodamine 6G and Mordant Blue 9, as model pollutants, under the visible and UV light. The composite catalysts presented much higher photocatalytic activity than pure TiO_2 under visible light and better photoefficiency than TiO_2 after exposure to UV light as well. The photodegradation reaction in the case of both azo dyes can be modeled assuming pseudo-first order kinetics. The mechanism of photocatalytic degradation has been discussed.

1. Introduction

Among semiconductor materials, titanium dioxide (TiO_2) in anatase phase has been shown as excellent and widely used photocatalyst for the degradation of different organic contaminants, because of its physical and chemical stability, high oxidative power, high catalytic activity, long-term photostability, low cost and ease of production. Many organic compounds can be decomposed in an aqueous solution in the presence of TiO_2, illuminated by photons with energies greater than or equal to the band gap energy of titanium dioxide (3.2 eV for anatase TiO_2) [1–6]. The major drawback for TiO_2 commercial use lies in its wide band gap, and relatively high recombination rate of photoinduced electron-hole pairs. The modification of TiO_2 by doping with metals and non-metals [7–12] or by Ti^{3+} self-doping [13,14] have been extensively performed in order to improve its photocatalytic activity under the visible irradiation.

Another very promising approach is the combination of TiO_2 with metal oxides like V_2O_5, ZnS, $InVO_4$, WO_3 [15-19] or graphene [20]. Among the metal oxides, WO_3 has smaller band gap (2.8 eV) than TiO_2 and better absorbs visible light. Moreover, WO_3 has a suitable conduction band potential and acts as a trapping site for photoexcited electrons from TiO_2.

The photogenerated holes from the valence band of WO_3 move towards and accumulate in the valence band of TiO_2. In such a way the efficiency of charge separation is increased, enhancing at the same time the photocatalytic acivity of TiO_2 [21]. Additionally, the formation of WO_x monolayer on TiO_2 increases the acidity of the TiO_2/WO_3 surface [22]. The higher acidity of TiO_2/WO_3 surface enables the adsorption of greater amount of hydroxyl groups and organic reactants on the surface [22, 23]. In recent years, TiO_2/WO_3 composites were synthesized using different methods such as sol-gel, ultrasonic spray pyrolysis, ball milling, hydrothermal, sol-precipitation, and impregnation to improve photocatalytic activity of TiO_2 under the visible light [24–28]. Thin films of TiO_2/WO_3 have also been prepared by dip and spin coating [29-31]. In most of these reports it was demonstrated that TiO_2/WO_3 composites were found to have much higher photocatalytic activity under the visible light than pure TiO_2 [25, 27, 28, 31]. Therefore, the combination of these two materials can lead to increased charge carrier lifetime and improved photocatalytic activity under the visible irradiation.

In the present work we used economic, efficient, and environmentally benign plasma electrolytic oxidation (PEO) process to synthetize TiO_2/WO_{3-x} coatings on titanium substrate. The structural, morphological, vibrational and optical properties of TiO_2/WO_{3-x} coatings were characterized by XRD, SEM, Raman and UV-vis spectroscopy. The photocatalytic efficiency of TiO_2/WO_{3-x} coatings was first tested under the visible light irradiation using model pollutant Rhodamine 6G and afterwards under UV light irradiation using Mordant Blue 9 as model pollutant. The mechanism of enhanced photocatalytic activity of TiO_2/WO_{3-x} composite coatings was also discussed.

2. Experimental section

2.1 Preparation of TiO_2/WO_{3-x} coatings

TiO_2/WO_{3-x} coatings were prepared on titanium substrate using plasma electrolytic oxidation (PEO) process. PEO process is an anodizing process of lightweight metals (aluminum, magnesium, zirconium, titanium, etc.) or metal alloys above the dielectric breakdown voltage, when thick, highly crystalline oxide coating with high corrosion and wear resistance, and other desirable properties are produced [32]. During the PEO process, numerous small sized and short-lived discharges are generated continuously over the coating's surface, accompanied by gas evolution. Due to increased local temperature, plasma-chemical reactions are induced at the discharge sites modifying the structure, composition, and morphology of such oxide coatings. The oxide coatings formed by PEO process usually contain crystalline and amorphous phases with constituent species originating both from metal and electrolyte. TiO_2/WO_{3-x} coatings were formed on the rectangular titanium samples (99.5% purity, Alfa Aesar) of dimensions 25 mm × 10 mm × 0.25 mm, which were used as working electrodes in the experiment. The working electrodes were sealed with insulation resin leaving only an area of 1.5 cm^2 as an active surface. Before starting the PEO process, titanium samples were degreased in acetone, ethanol, and distilled water, using ultrasonic cleaner and dried in a warm air stream. The anodic oxidation process was conducted in an aqueous solution of 10^{-3} M 12-tungstosilicic acid ($H_4SiW_{12}O_{40}$), at constant current density (150 mA/cm^2). During PEO process, the electrolyte circulated through the chamber–reservoir system. The temperature of the electrolyte was kept fixed at (20 ± 1) ^0C. Detailed description of PEO process is given in the ref. [33].

After plasma electrolytic oxidation, the samples were rinsed in distilled water to prevent additional deposition of electrolyte components during drying. The TiO_2/WO_{3-x} samples were

obtained by varying the time of PEO process from 90 s up to 300 s. The pure TiO_2 sample was obtained after 300 s of PEO process.

2.2 Characterization of TiO_2/WO_{3-x} coatings

The crystal structure of TiO_2/WO_{3-x} samples was analyzed by X-ray diffraction (XRD), using a Rigaku Ultima IV diffractometer in Bragg-Brentano geometry, with Ni-filtered CuKα radiation (λ=1.54178 Å). Diffraction data were acquired over the scattering angle 2θ from 15^o to 75^o with a step of 0.02^o and acquisition rate of 2^o/min.

Scanning electron microscope (SEM) JEOL 840A was used to characterize the morphology of formed oxide coatings.

Micro-Raman scattering measurements were performed at room temperature in a backscattering geometry, using a Jobin-Yvon T64000 triple spectrometer system and Nd:YAG laser line of 532 nm as an excitation source. The incident laser power was kept less than 10 mW in order to prevent the heating effects.

UV-vis diffuse reflectance spectra were acquired using the Specord M40 Carl Zeiss spectrometer.

2.3 Photocatalytic experiments

The photocatalytic activity of TiO_2/WO_{3-x} samples was evaluated by monitoring the decomposition of Rhodamine 6G (R6G) and Mordant Blue 9 (MB9) under the irradiation of two different light sources: fluorescent and UV lamps. The photocatalytic measurements on R6G solution (initial concentration in water: 1 mg/L) have been performed at initial pH=7, using a 36 W visible fluorescent lamp (Hyundai eagle) [9]. The cuvette (3 mL) was placed at about 5 cm from the lamp. The evolution of the rhodamine concentration was followed by measuring the variation of the intensity of main absorption peak at ~525 nm. UV-vis absorption measurements as a function of the light exposure time were performed by using USB2000 spectrometer by Ocean Optics. The solution was placed in the dark for 60 minutes to reach the adsorption/desorption equilibrium before visible light exposure.

The photocatalytic activity of TiO_2/WO_{3-x} samples under UV light irradiation was evaluated using aqueous solution of Mordant Blue 9 (MB9) as a model pollutant. Batch type experiments were performed in an open termostated cell (at 25 °C). The cell was equipped with a water circulating jacket to maintain the solution at room temperature. A mercury lamp (125 W) was used as a light source and was placed 13 cm above the surface of the dye solution. The initial concentration of MB9 in an aqueous suspension was 50 mg/L and the working volume was 25 mL. The experiments were carried out at pH=6 of the suspension which did not vary during the degradation process. Before the lamp was switched on, the cell was kept in dark for 60 minutes in order to achieve the adsorption-desorption equlibrium. At regular time intervals the aliquots were taken and the concentration of the dye was determined by UV-vis spectrophotometer (Super Scan) at λ_{max}=516 nm. All photocatalytic measurements were repeated at least twice to check their reproducibility.

3. Results and discussion

3.1 Crystal structure and morphology

XRD diffraction patterns of the TiO_2/WO_{3-x} samples obtained for 90 (TW90), 120 (TW120), and 300 s (TW300) of PEO process are presented in Fig. 1. According to the JCPDS data, the major diffraction peaks at $2\theta = 23.32^0$, 33.34^0, 41.34^0, 54.28^0 and 59.91^0 can be indexed to the structure of monoclinic $W_{18}O_{49}$ ($WO_{2.72}$) phase, suggesting that TiO_2/WO_{3-x}

coatings are not fully oxidized. Besides the intense XRD peaks which belong to monoclinic phase, small peaks at 25.3^0 and 48.1^0 of anatase TiO_2 phase (marked as A on Fig. 1) and peaks of elemental Ti were visible in the XRD patterns of TiO_2/WO_{3-x} samples. With increasing duration of PEO process intensities of XRD peaks which belong to elemental Ti decreased implying an increase of TiO_2/WO_{3-x} coating. At the same time, the XRD peaks of monoclinic WO_{3-x} phase became more intense, indicating that the TiO_2/WO_{3-x} coatings were enriched with WO_{3-x} crystal phase. The crystallite size was determined only for WO_{3-x} phase, because of low intensity of anatase peaks which overlap with intense WO_{3-x} peaks [34]. The average crystallite size for TW90 samples was 15 nm and with increasing PEO time the average crystallite size decreased to 11 nm for TW300 sample [34].

Fig. 1

In Fig. 2 are presented SEM images of TiO_2/WO_{3-x} samples. In the TW90 sample produced with shorter PEO time, certain number of microdischarge channels together with molten regions were present because of the rapid cooling of the electrolyte. With increasing time of PEO process, when the thickness of the oxide coating was increased, the number of microdischarge channels and micropores decreased followed by increased roughness of the coating's surface [34].

Fig. 2

3.2 Raman and diffuse reflectance spectra

The Raman spectra of TiO_2/WO_{3-x} samples produced for different duration of PEO process are shown in Fig. 3a. Several modes originating from two crystalline oxide phases can be identified (marked on Fig. 3a as T and W).

Fig. 3

The Raman modes positions were determined using Lorentzian fit procedure and the deconvoluted spectra of TW90, TW120 and TW300 samples are presented in the Fig. 3b. Besides the modes at about 144 cm^{-1} ($E_{g(1)}$), 197 cm^{-1} ($E_{g(2)}$), 393 cm^{-1} ($B_{1g(1)}$), 516 cm^{-1} (A_{1g}, $B_{1g(2)}$) and 638 cm^{-1} ($E_{g(3)}$) which belong to anatase phase of TiO_2 [35], several modes characteristic for monoclinic WO_{3-x} phase are present [23, 36, 37]. The broad band at ~703 cm^{-1} and strong band at ~793 cm^{-1} are assigned to the stretching (O–W–O) modes of the bridging oxygen of the WO_6 octahedra. The bands observed at ~272 cm^{-1} and at ~316 cm^{-1} are assigned to the bending (O–W–O) vibrations of bridging oxygen in monoclinic m-WO_3 [23, 37]. The band positioned at ~989 cm^{-1} is assigned to the dioxo $(W=O)_2$ symmetric vibration of the isolated surface WO_4 structure, whereas its weak shoulder at ~942 cm^{-1} represents asymmetric vibration of the same atomic group [23, 37]. The low frequency mode at 58 cm^{-1} belongs to the to lattice modes of monoclinic WO_3 phase [38].

Further, from the Lorentzian fit procedure it was obtained that the ratio between the intensity of the peak positioned at 639 cm^{-1} and sum of the intensities of the 703 cm^{-1} and 793 cm^{-1} peaks decreased with the increase of PEO time. This fact supports the XRD results that WO_{3-x} content increases with prolonged PEO process duration.

In Fig. 4 are presented the Raman spectra of TW90, TW120 and TW300 samples in the C–H and O–H region. The Raman band at around 2885 cm^{-1} originates from the overlapped CH_3 and CH_2 stretching vibrations [39]. Broad Raman peak in the 3000-3600 cm^{-1} frequency

range can be assigned to the O–H stretching vibration of water molecules adsorbed on the surface of the TiO_2/WO_{3-x} coatings [3, 5].

Fig. 4

The absorbance spectra of TW90, TW120 and TW300 samples are given in Fig. 5a. With increasing content of WO_{3-x} phase the absorption edge shifts to higher wavelengths. In the spectra of TW120 a structure around 380-400 nm can be observed, which is very pronounced in the TW300 sample. The appearance of this absorption structure can be attributed to the electronic population of WO_3 conduction band [40]. From the absorption spectra from Fig. 4a, applying the same procedure as Ghobadi in his work [41], the band gap energies for pure TiO_2 and TiO_2/WO_{3-x} samples were estimated. In Fig. 5b are presented the Tauc plots for indirect transition, as TiO_2 and WO_3 are indirect band gap semiconductors [27]. The band gap (E_g) energies are 3.19 eV for pure TiO_2, and 2.84, 2.77 and 2.6 eV for TW90, TW120 and TW300 samples, respectively. It is obvious that with increasing WO_{3-x} content the band gap decreases compared to pure TiO_2 and shifts to the visible spectral range. Patrocinio et al. [40] have shown that in TiO_2/WO_3 films, the WO_3 conduction band introduces new low lying electronic levels with respect to the conduction band of TiO_2, causing the lowering of the band gap energy of composite samples compared to pure TiO_2. This finding is in accordance with the band gap behavior of TiO_2/WO_{3-x} samples from Fig. 5b.

Fig. 5

3.3 Photocatalytic performances of TiO_2/WO_{3-x} coatings

Fig. 6a shows the kinetics of degradation of R6G for pure TiO_2, TW90, TW120 and TW300 samples under the visible light. No detectable degradation of R6G was registered without the presence of TiO_2/WO_{3-x} samples (black circles on Fig. 6a). As can be seen from Fig. 6a, the TiO_2 and TiO_2/WO_{3-x} samples adsorbed the dye in the equilibrium period of 60 minutes before the exposure to visible light. It is known from the literature that the zero point charge (pH_{zpc}) of TiO_2 lies between 6 and 6.8, and at lower pH values the TiO_2 surface is positively charged [42, 43, 44]. The adsorption of the R6G as cationic dye at pH=7, points out that at this pH value the surfaces of TiO_2 and TiO_2/WO_{3-x} samples are negative and attract the positively charged R6G. The dye adsorption ability can be decisive reason for the high catalytic activity of the catalyst, because it can enhance the electron/hole transfer efficiency and contact with photogenerated active species.

When TiO_2 and TiO_2/WO_{3-x} samples were subjected to visible radiation, TiO_2/WO_{3-x} samples showed much better photoefficiency and demonstrated to be far superior to that of pure TiO_2. The highest activity was observed for the TW90 sample for which the photodegradation percent for R6G reached almost 80% after 60 minutes. With increasing content of WO_{3-x}, the photocatalytic efficiency slightly decreased, but is still higher than for pure TiO_2.

Fig. 6

Further, the photocatalytic activity of TiO_2/WO_{3-x} samples for degradation of MB9 was tested under the UV light. In Fig. 6b is presented the photodegradation of MB9 in the presence of TiO_2/WO_{3-x} samples. In the dark, TiO_2/WO_{3-x} samples showed no adsorption of MB9, because the pH value of MB9 solution (pH=6) was close to the pH_{zpc} of TiO_2 and the electrostatic attraction between MB9 dye molecules and TiO_2 or TiO_2/WO_{3-x} surfaces is

expected to be weak. The photocatalytic activity of TiO_2/WO_{3-x} samples was improved with increased content of WO_{3-x} phase, so the TW300 sample exhibited the best activity among the rest of the samples. As can be seen from Fig. 6b, after 240 minutes more than 80% of dye was degraded.

Photocatalytic degradation of both dyes can be well described by first-order kinetic equation, $ln(C/C_o)=kt$, where C_o is the initial dye concentration and C is the dye concentration at time t. The first order kinetic constant k is obtained from the slope of the $ln(C/C_o)$ versus t for both dyes. In the Table 1 are given the first order rate constants for R6G and MB9 (k_{R6G}, k_{MB9}), together with the corresponding linear correlation coefficient (R^2). In a case of R6G degradation under the visible light, the highest k value (k_{R6G}) was obtained for the TW90 sample. In a case of MB9 degradation under UV light, value of k_{MB9} increased with increasing amount of WO_3. Comparing the k_{R6G} and k_{MB9} values from Table 1, it can be concluded that the photoactivity of TiO_2/WO_{3-x} samples under the visible irradiation is higher than under UV irradiation. Furthermore, the photoactivity of TiO_2/WO_{3-x} samples is always higher than that of pure TiO_2.

Table 1. The pseudo-first rate constants for R6G and MB9 together with R^2.

Sample	$k_{R6G} \times 10^{-2}$ (min^{-1})	R^2	$k_{MB9} \times 10^{-2}$ (min^{-1})	R^2
TW90	1.52	0.975	0.44	0.990
TW120	1.24	0.957	0.47	0.982
TW300	1.20	0.963	0.65	0.966
TiO_2	0.28	0.888	0.41	0.963

3.4 Mechanism of the reaction

The photocatalytic degradation of R6G and MB9 is initiated by the photoexcitation of the TiO_2/WO_{3-x} coatings when the electron-hole pairs are formed on the catalyst's surface. The absorption measurements have shown that the band gap energy of TiO_2 is higher than that of TiO_2/WO_{3-x} coatings and with increasing WO_{3-x} content the band gap decreases and shifts to the visible spectral range.

According to the generally accepted photoexcitation mechanism, electrons from the conduction band of TiO_2 can easily diffuse into the conduction band of WO_3. Since W(VI) can be easily reduced to W(V), WO_3 acts as an acceptor of conduction band electrons from TiO_2, whereas the photogenerated holes migrate in the opposite direction, i.e. from the lower-lying valence WO_3 band to the valence band of TiO_2. In such a way the charge separation efficiency can be increased. As the conduction band of WO_{3-x} is lower with respect to WO_3 and TiO_2, the presence of WO_{3-x} will further reduce the band gap of TiO_2/WO_{3-x} samples [45] increasing the charge carriers lifetime. As a result, the electron-hole recombination will be more difficult and more reacting radicals can be produced at the TiO_2/WO_{3-x} surface.

Fig.7

In Fig. 7 is given an illustration of photo-induced electron-hole separation and reacting radicals formation. The presence of holes in the dye solution permits a direct oxidation of the dye, due to high oxidative potential of the holes (h^+):

$$h^+ + \text{dye} \rightarrow \text{dye}^{\bullet+} \rightarrow \text{oxidation of the dye} \quad (1)$$

Further, hydroxyl radicals ($OH^{\bullet}$) are usually formed by the reaction between the holes/electrons and water molecules or OH^- present on the surface of the catalyst [28]. The $OH^{\bullet}$ radicals attack the dye in aqueous solution leading to its degradation:

$$OH^{\bullet} + \text{dye} \rightarrow \text{photodegradation of the dye} \quad (2)$$

The electrons can react with dissolved oxygen to form superoxide ions ($O_2^{-\bullet}$) which react with H_2O molecules forming OH^- ions and finally $OH^{\bullet}$ radicals.

It is known from the literature that WO_3 is is almost 15 times more acidic than TiO_2 [22, 23, 31], so it is expected that the surface of TiO_2/WO_{3-x} samples is more acidic than that of TiO_2, and has a higher affinity for chemical species having unpaired electrons. Because of higher acidity, the surface of TiO_2/WO_{3-x} composites can absorb more H_2O and OH^- and generate more $OH^{\bullet}$ radicals [22, 23]. The Raman spectra of TiO_2/WO_{3-x} coatings presented in Fig. 4, gave an evidence that adsorbed H_2O and hydroxyls are present on their surface, existence of which is important for the formation of $OH^{\bullet}$ radicals.

It is worth mentioning that TiO_2/WO_{3-x} samples exhibited better photocatalytic activity under the visible light than under UV light for the same irradiation time. Namely, after 60 minutes of degradation process, more than 70% of R6G and only 40% of MB9 is removed from the solution. This is expected if we have in mind that WO_{3-x} absorbs in the visible region (E_g<2.8 eV) and therefore should be more efficient as catalyst under the visible light. Slight decrease of photocatalytic activity of TW300 sample in a case of R6G photodegaradation (Fig. 6a) can be explained by the occurrence of photochromism [28, 40]. Namely, the electron accumulation at the WO_3 conduction band can be more pronounced with increased WO_3 content. The accumulated electrons can react with $OH^{\bullet}$ radicals forming OH^- ions or can reduce the number of superoxide radicals [28, 40] degrading at some extent the photocatalytic activity of TiO_2/WO_{3-x} coatings. The presence of pronounced absorption feature around 380-400 nm in the absorbance spectrum of TW300 sample confirms this assumption.

4. Conclusion

TiO_2/WO_{3-x} composite and pure TiO_2 coatings have been prepared on titania substrates using facile and cost-effective plasma electrolytic oxidation process. The structural, morphological, vibrational and absorption properties of these samples were investigated by different methods such as XRD, SEM, Raman and absorption spectroscopy. XRD and Raman analysis revealed that the coatings are partially crystallized and mainly composed of monoclinic WO_{3-x} and anatase TiO_2. The crystallinity of the samples was improved with increasing amount of WO_{3-x} phase. The presence of WO_{3-x} phase caused a decrease of optical band gap, i.e. shift from near UV to visible spectral region. The photocatalytic activity of TiO_2/WO_{3-x} samples has been evaluated for the degradation of two different model pollutants in an aqueous solution, R6G under visible and MB9 under UV light irradiation. The TiO_2/WO_{3-x} samples have shown much higher degradation rate of R6G under the visible light irradiation than that of pure TiO_2 synthesized under the same condition. Under the UV light, the TiO_2/WO_{3-x} photocatalysts have shown better photocatalytic activity for the degradation of MB9 than pure TiO_2. The kinetics of the reaction in the case of both azo dyes followed the pseudo first order. The enhanced photocatalytic activity is attributed to better light absorption and increased charge separation efficiency of the TiO_2/WO_{3-x} samples. The significant amount of adsorbed H_2O and hydroxyls present on TiO_2/WO_{3-x} surface is the prerequisite for

the generation of $OH^{\bullet}$ radicals. The TiO_2/WO_{3-x} samples exhibit higher affinity for chemical species having unpaired electrons and behave as much better photocatalysts than pure TiO_2.

Acknowledgements

This work was financially supported by the Ministry of Education, Science and Technological Development of the Republic of Serbia under the projects ON171032 and III45018.

References

[1] L. Ren, Y. Li, J. Hou, X. Zhao, and C. Pan, ACS Appl. Mater. Interfaces 6 (2014) 1608−1615.
[2] F. Ruggieri, A. A. D'Archivio, M. Fanellia, S. Santucci, RSC Adv. 1 (2011) 611–618.
[3] M. Šćepanović, B. Abramović, A. Golubović, S. Kler, M. Grujić-Brojčin, Z. Dohčević-Mitrović, B. Babić, B. Matović, Z. V. Popović, J. Sol-Gel Sci. Technol. 61 (2012) 390–402.
[4] A. Golubović, B. Abramović, M. Šćepanović, M. Grujić-Brojčin, S. Armaković, I. Veljković, B. Babić, Z. Dohčević-Mitrović, Z.V. Popović, Mater. Res. Bull. 48 (2013) 1363‑1371.
[5] S. Watson, D. Beydoun, J. Scott, R. Amal, J. Nanoparticle Res. 6 (2004) 193–207.
[6] A. N. Banerjee, Nanotechnol. Sci. Appl. 4 (2011) 35–65.
[7] M. Xing, D. Qi, J. Zhang, F. Chen, Chem. Eur. J. 17 (2011) 11432–11436.
[8] Y. Niu, M. Xing, J. Zhang, B. Tian, Catal. Today 201 (2013) 159– 166.
[9] F. Ruggieri, D. Di Camillo, L. Maccarone, S. Santucci, L. Lozzi, J. Nanopart. Res. 15 (2013) 1-11.
[10]M. Xing, W. Li, Y. Wu, J. Zhang, X. Gong, J. Phys. Chem. C 115 (2011) 7858–7865.
[11] M. Janus, B. Tryba, E. Kusiak, T. Tsumura, M. Toyoda, M. Inagaki, A. W. Morawski, Catal. Lett. 128 (2009) 36–39.
[12] M. Takeuchi, M. Matsuoka, M. Anpo, Res. Chem. Intermed. 38 (2012) 1261–1277.
[13] X. Chen, L. Liu, P.Y. Yu, S.S. Mao, Science 331 (2011) 746–750.
[14] W. Fang, M. Xing, J. Zhang, Appl. Catal. B: Environ. 160–161 (2014) 240–246.
[15] Y. Wang, J. Zhang, L. Liu, C. Zhu, X. Liu, Q. Su, Mater. Lett. 75 (2012) 95–98.
[16] Y. Xiaodan, W. Qingyin, J. Shicheng, G. Yihang, Mat. Charac. 57 (2006) 333–341.
[17] J. Rashid, M. A. Barakat, S. L. Pettit, J. N. Kuhn, Environ. Technol. 35 (2014) 2153-2159.
[18] B. Gao, Y. Ma, Y. Cao, W. Yang, J. Yao, J. Phys. Chem. B 110 (2006) 14391–14397.
[19] X. Luo, F. Liu, X. Li, H. Gao, G. Liu, Mat. Sci. Semicon. Proc. 16 (2013)1613–1618.
[20] N. R. Khalid, E. Ahmed, Z. Hong, M.Ahmad, Y. Zhang, S. Khalid, Ceram. Int. 39 (2013) 7107–7113.
[21] Y. Li, P. C. Hsu, S. M. Chen, Sensor. Actuat. B-Chem. 174 (2012) 427– 435.
[22] Y. T. Kwon, K. Y. Song, W. I. Lee, G. J. Choi, Y. R. Do, J. Catal. 191 (2000) 192–199.
[23] K. K. Akurati, A. Vital, J. P. Dellemann, K. Michalowa, T. Graule, D. Ferri, A. Baiker, Appl. Catal. B: Environ. 79 (2008) 53–62.
[24] D. Ke, H. Liu, T. Peng, X. Liu, K. Dai, Mater. Lett. 62 (2008) 447–450.
[25] H. Song, H. Jiang, X. Liu, G. Meng, J. Photoch. Photobio. A 181 (2006) 421–428.
[26] C. Shifu, C. Lei, G. Shen, C. Gengyu, Powder Technol. 160 (2005) 198–202.
[27] F. Riboni, L. G. Bettini, D. W. Bahnemann, E. Selli, Catal. Today 209 (2013) 28– 34.

[28] J. Yang, X. Zhang, H. Liu, C. Wang, S. Liu, P. Sun, L. Wang, Y. Liu Catal. Today 201 (2013) 195– 202.
[29] T. Tatsuma, S. Takeda, S. Saitoh, Y. Ohko, A. Fujishima Electrochem. Commun. 5 (2003) 793–796.
[30] A. Rampaul, I. P. Parkin, S. A. O'Neill, J. DeSouza, A, Mills, N. Elliott, Polyhedron 22 (2003) 35-44.
[31] J. H. Pan, W. In Lee, Chem. Mater. 18 (2006) 847-853.
[32] A. L. Yerokhin, X. Nie, A. Leyland, A. Matthews, S. J. Dowey, Surf. Coat. Technol. 122 (1999) 73-93.
[33] S. Stojadinović, N. Radić, R. Vasilić, M. Petković, P. Stefanov, Lj. Zeković, B. Grbić Appl. Catal. B: Environ. 126 (2012) 334– 341.
[34] L. J. Rožić, S. Petrović, N. Radić, S. Stojadinović, R. Vasilić, P. Stefanov, B. Grbić, Thin Solid Films 539 (2013) 112–116.
[35] T. Ohsaka, F. Izumi, Y. Fujiki, J. Raman Spectrosc. 7 (1978) 321–324.
[36] Y. Djaoued, S. Balaji, N, Beaudoin, J. Sol-Gel Sci. Technol. 65 (2013) 374–383.
[37] C. Santato, M. Odziemkowski, M. Ulmann, Jan Augustynski, J. Am. Chem. Soc. 123 (2001) 10639-10649.
[38] E. Cazzanelli, C. Vinegoni, G. Mariotto, A. J. Purans Solid State Ionics 123 (1999) 67–74.
[39] Y. Yu, K. Lin, X. Zhou, H. Wang, S. Liu, X. Ma, J. Phys. Chem. C 111 (2007) 8971-8978.
[40] A. O. T. Patrocinio, L. F. Paula, R. M. Paniago, J. Freitag, D. W. Bahnemann, ACS Appl. Mater. Interfaces 6 (2014) 16859−16866.
[41] N. Ghobadi, Int. Nano Let. 3 (2013) 1-4.
[42] A. A. Khodja, A. Boulkamh, C. Richard, Appl. Catal. B: Environ. 59 (2005) 147–154.
[43] C. C. Wang, J. Y. Ying, Chem. Mater. 11 (1999) 3113–3120.
[44] M. D. Hernández-Alonso, F. Fresno, S. Suarez, J. M. Coronado, Energy Environ. Sci. 2 (2009) 1231–1257.
[45] A. K. L. Sajjad, S. Shamaila, B. Tian, F. Chen, J. Zhang, Appl. Catal. B: Environ. 91 (2009) 397–405.

Figure 1

Click here to download high resolution image

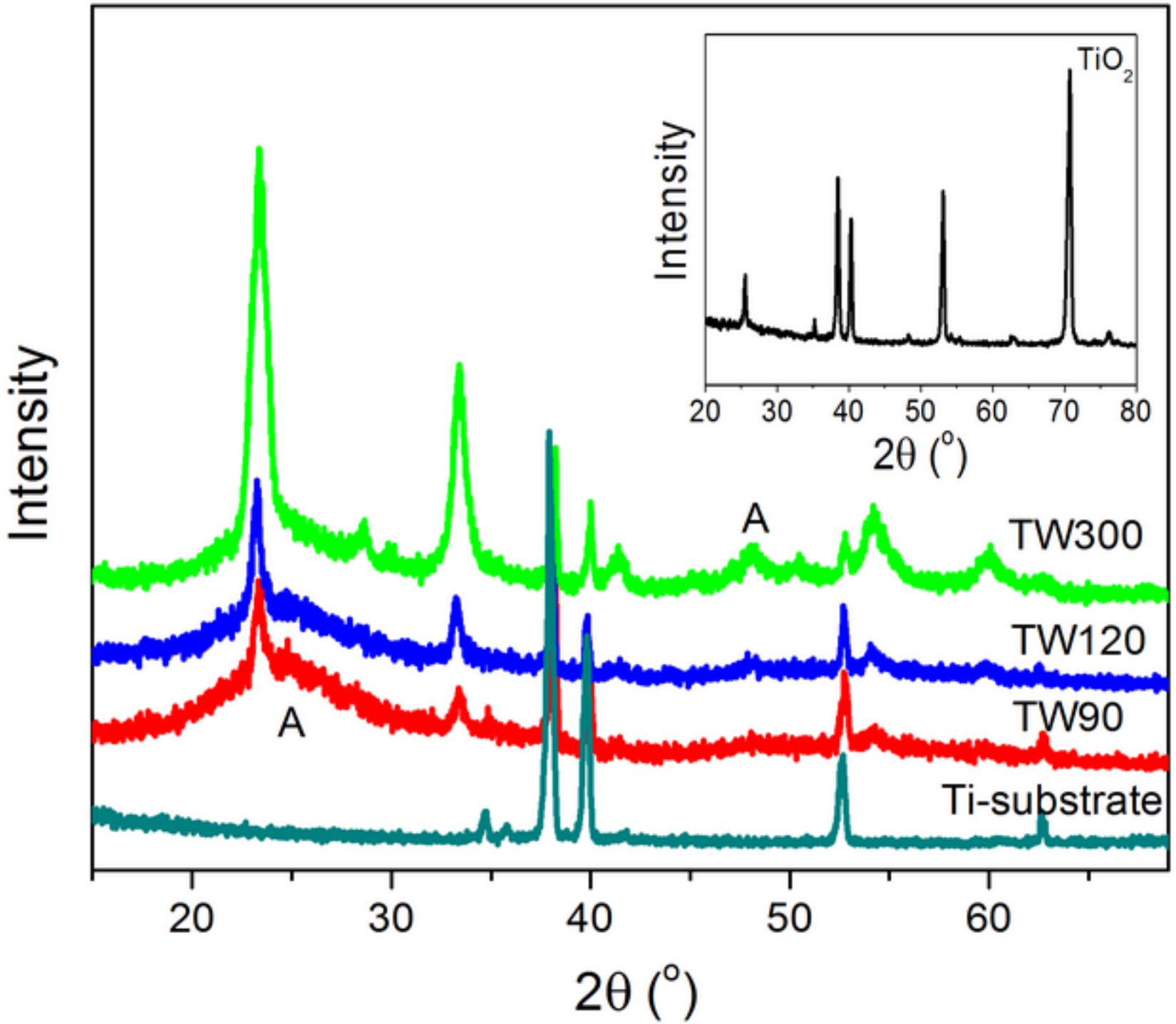

Figure 2

Click here to download high resolution image

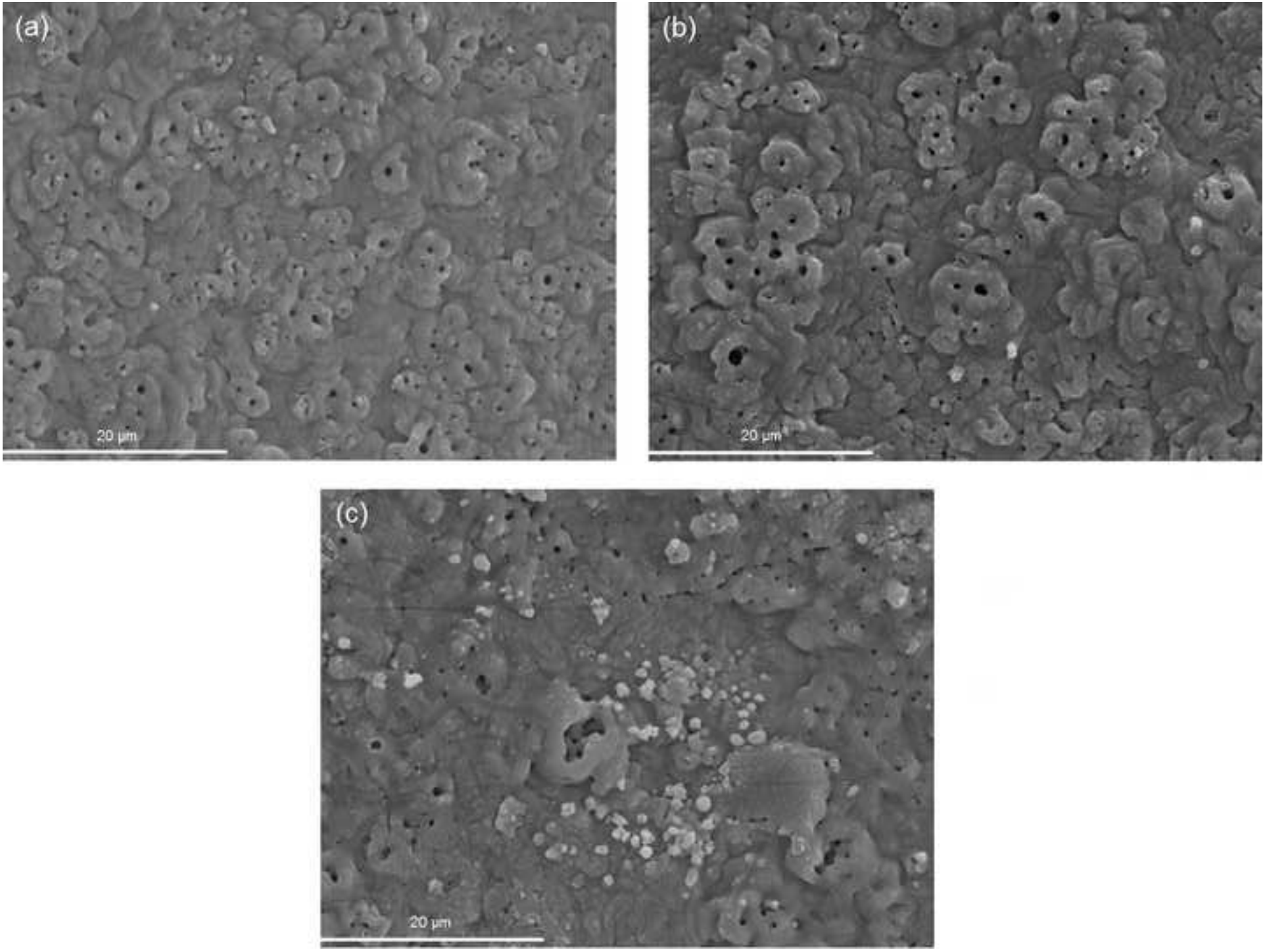

Figure 3

Click here to download high resolution image

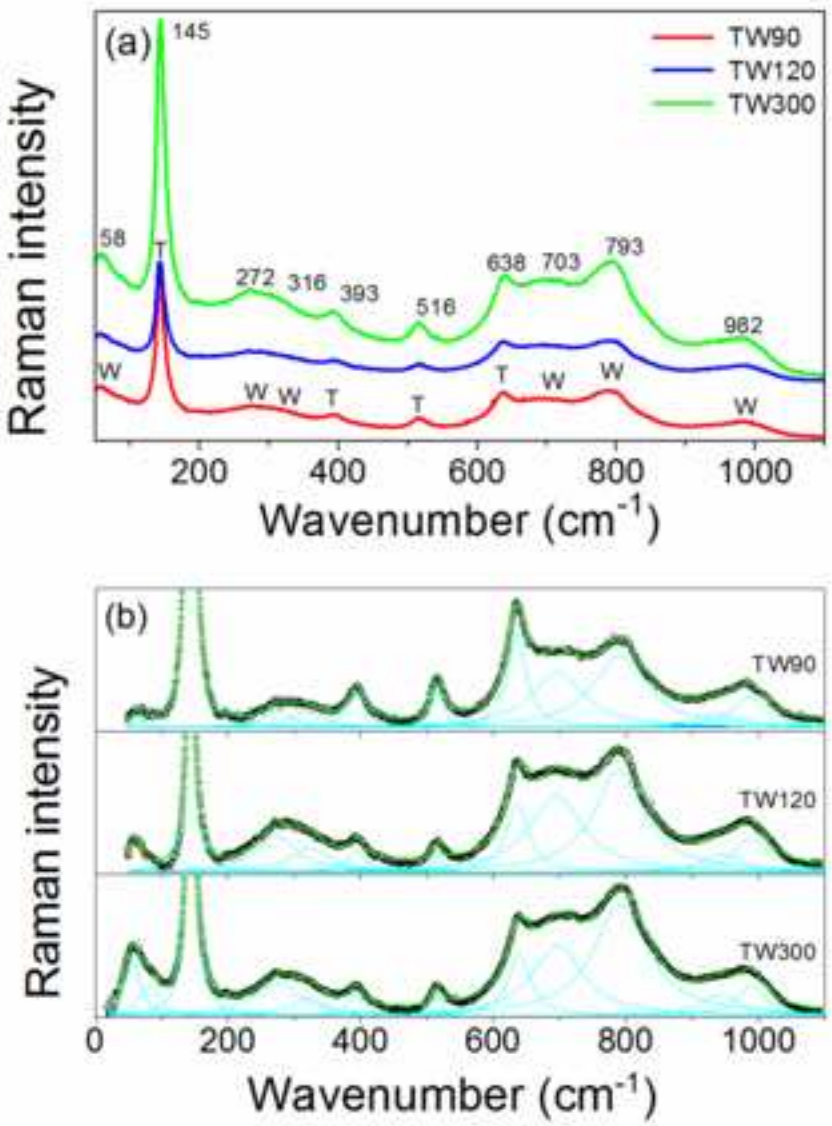

Figure 4

Click here to download high resolution image

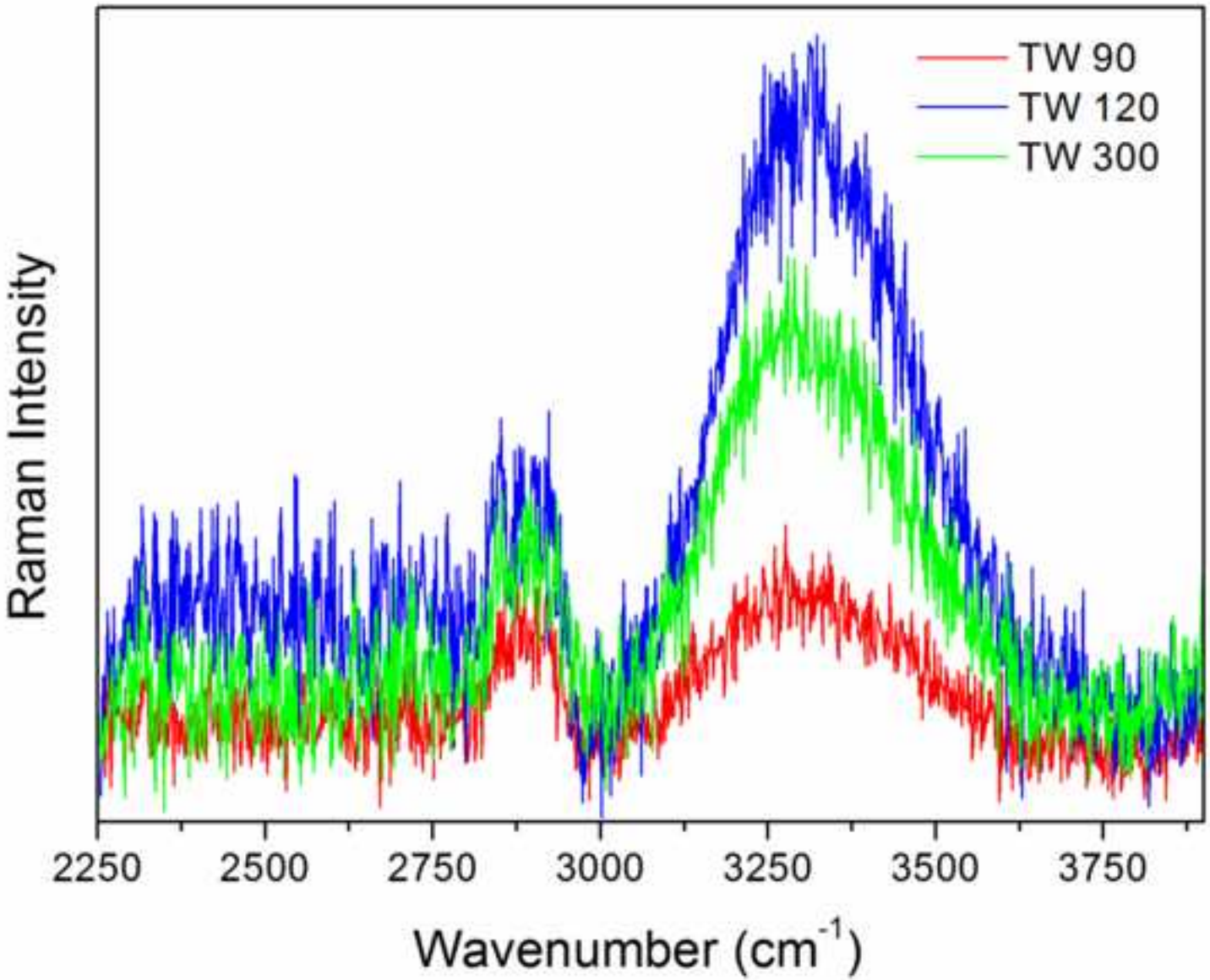

Figure 5

Click here to download high resolution image

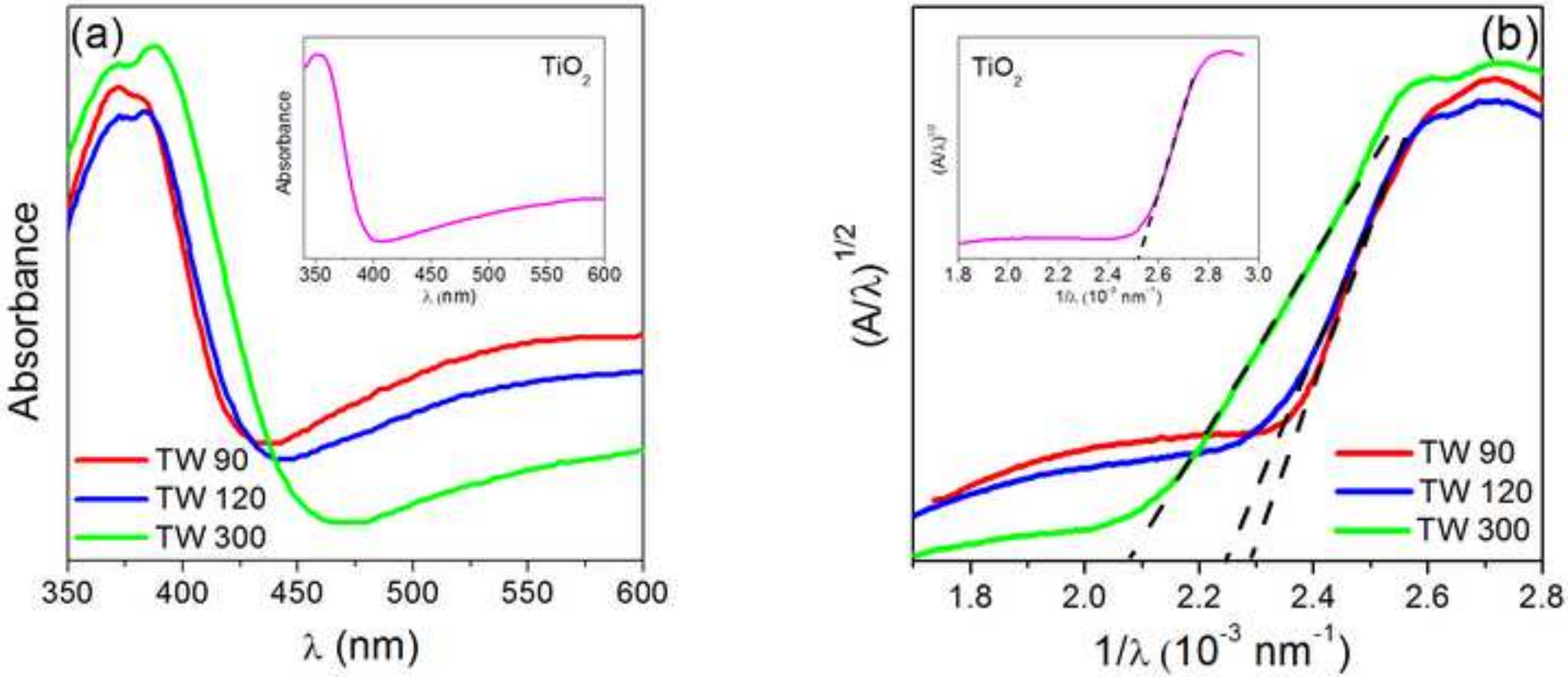

Figure 6

Click here to download high resolution image

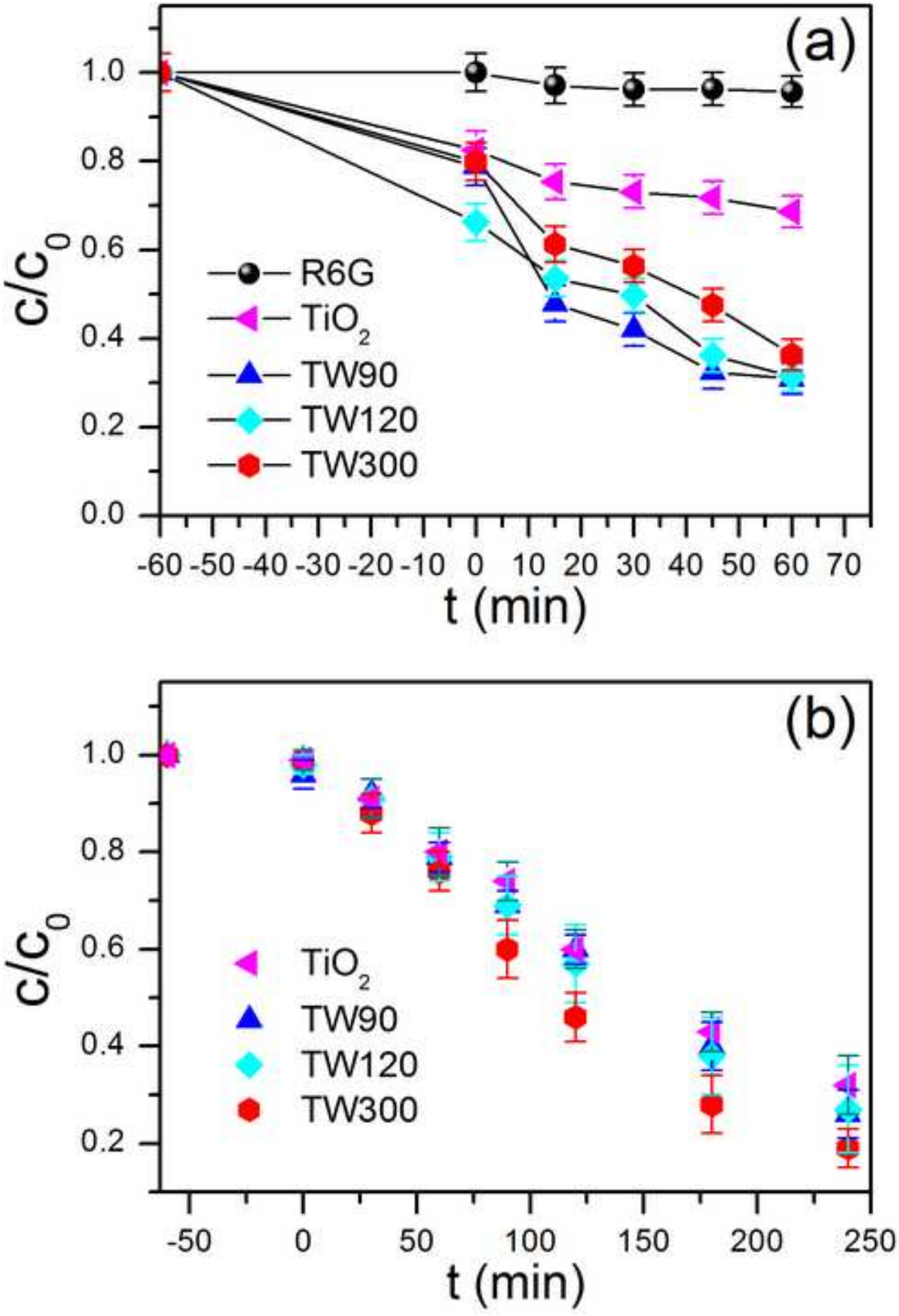

Figure 7

Click here to download high resolution image

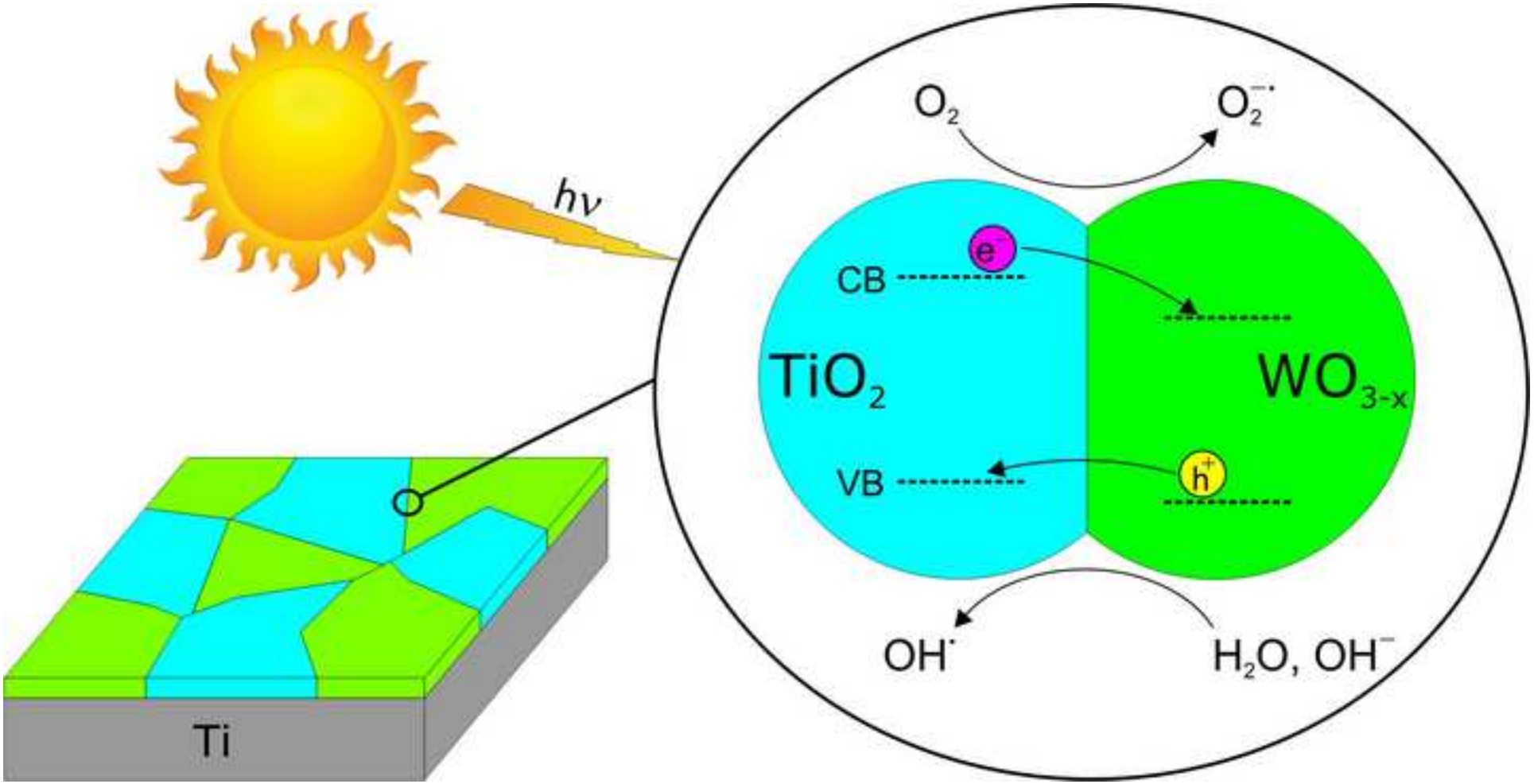

*Graphical Abstract

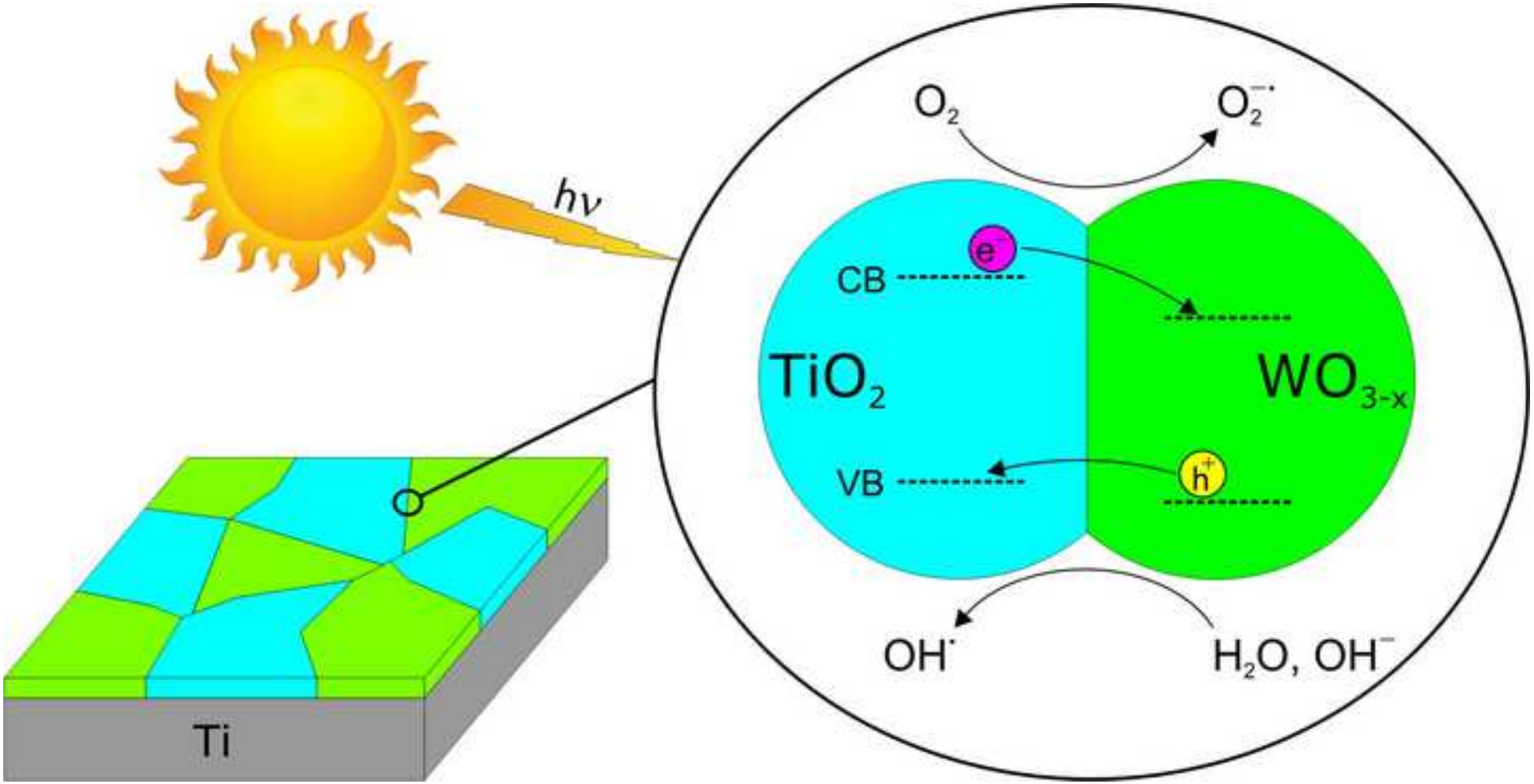

Highlights

- TiO_2/WO_{3-x} coatings were fabricated via plasma electrolytic oxidation process.
- Catalysts exhibited better photocatalytic activity under UV light than TiO_2.
- Visible-light degradation activity of catalysts is enhanced compared to UV light.
- Catalysts exhibit better light absorption and slow down the recombination process.